6

Biophysical Considerations of Membrane Electroporation

Eberhard Neumann, Andreas Sprafke, Elvira Boldt, and Hendrik Wolf
Faculty of Chemistry, University of Bielefeld, D-4800 Bielefeld 1, Germany

I. Introduction

Membrane electroporation describes the transient, reversible permeabilization of the membranes of cells, organelles, or lipid bilayer vesicles by electric field pulses; for review see Neumann *et al.* (1989). Electroporation not only renders membranes transiently permeable and leads to material exchange across membranes, but also induces and facilitates fusion of membranes in contact; for review see Sowers (1987). There is an increasing number of practical applications of the electroporation technique, for instance:

Guide to Electroporation and Electrofusion

- Direct transfer of genes, other nucleic acids, proteins, and other molecules into all types of cells and microorganisms.
- Electrofusion of cells.
- Electrostimulation of cell growth and proliferation.
- Electroinsertion of membrane proteins.

Contrary to the impressive success of the electroporation techniques in cell biology, biotechnology, and medicine (gene therapy), the molecular membrane processes of electroporation are not yet well understood. Data analysis and optimization of conditions for the electrotransfer of DNA and of proteins, electrofusions, electrostimulation, and electroinsertion are still primarily empirical.

Since it is primarily the lipid part of biological membranes that is electroporated, lipid bilayer vesicles may be used as a model system to study the elementary processes of the electroporation phenomena.

Recent electrooptic and conductometric data are consistent with electric field-induced changes in the membrane structure of the vesicles. The lipids rearrange in such a way that optically anisotropic light scattering centers appear in the lipid phase of the vesicles. These scattering centers may be identified with geometrically anisotropic pores, which conduct alkali salt ions and other substances if, at given field strengths and pulse durations, a critical pore size is reached.

The relaxation kinetic data are the basis for the interpretation of a variety of observations accumulated in previous studies on membrane permeabilization, cell electrotransfection, and electrofusion. Deeper insight is gained on the stimulus/duration curve, on the electrosensitivity of cells, on the dependences of cell transformations on DNA and cell concentrations, and various other parameters.

II. Electrooptic and Conductometric Relaxations of Lipid Bilayer Vesicles

Recent progress in relaxation kinetics in the presence of high electric field strengths has provided new ways to study structural changes in membrane systems. We have developed an electric field-jump relaxation spectrometer that permits the simultaneous measurements of field pulse-induced changes in electric conductance and in optical properties of solutions and suspensions in the nanosecond to millisecond time range with high resolution. Rectangular field pulses up to 150 kV cm^{-1} and of variable pulse duration (0.5 μs to 1 ms) can be applied by cable discharge in a single DC-pulse mode.

A. Relaxation Data

Figure 1 shows that there are up to three conductance modes $\Delta\lambda/\lambda(0)$ and up to two electrooptic scattering–dichroitic relaxation modes.

Mode I of the conductance relaxation clearly has the feature of a displacement current, as expected for the interfacial ionic polarization preceding, as an exponen-

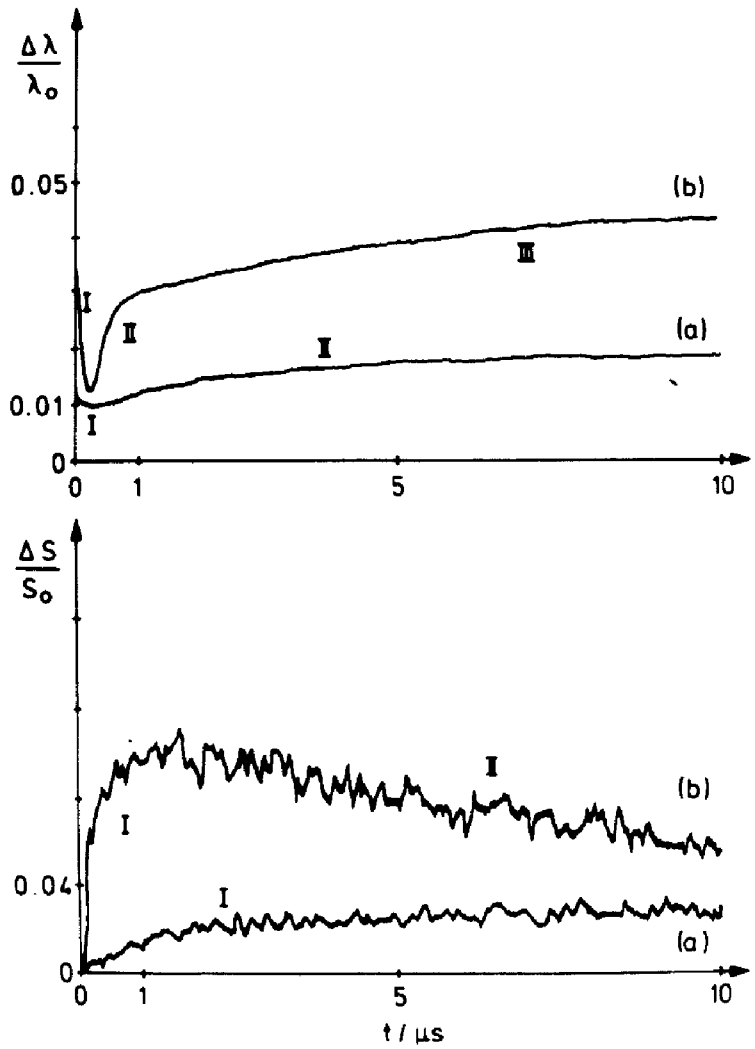

Figure 1 Conductometric ($\Delta\lambda/\lambda_0$) and electrooptic ($\Delta S/S_0$) relaxations of a turbid 0.2 m*M* NaCl suspension of lipid bilayer vesicles (mean diameter $\theta = 80 + 20$ nm) filled with 0.2 m*M* NaCl, pH 6.6, 20°C. Vesicle density: 10^{12}/ml (= 0.5 m*M* lipid). Time courses of the relative conductivity $\Delta\lambda/\lambda(0)$ and of the relative scattering dichroism at 332 nm light wavelength in the presence of a constant electric field strength E and of $\Delta t = 10$ μs duration: (a) $E = 20$ kV cm^{-1} and (b) $E = 60$ kV cm^{-1}; $\lambda(0) = 22.6$ μS cm^{-1} at 20°C. The Roman numerals refer to the (exponential) relaxation modes.

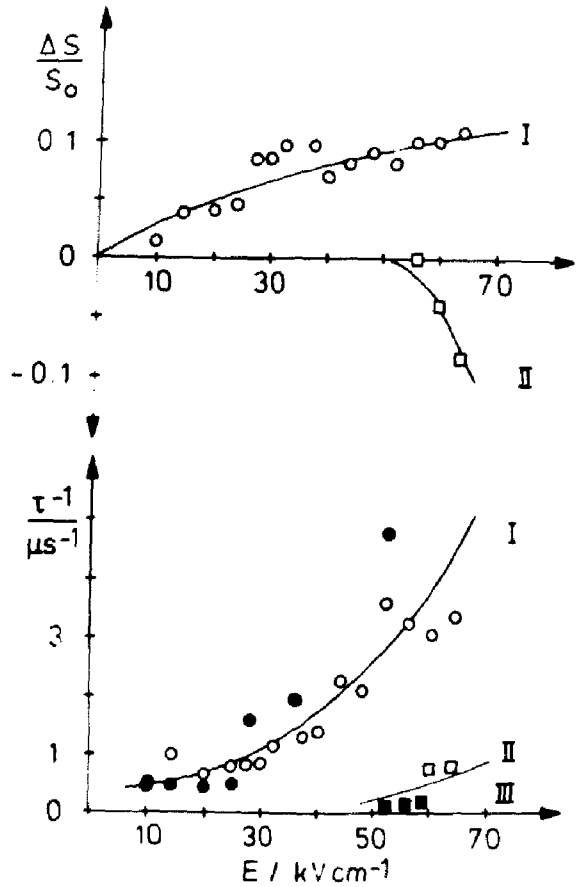

Figure 2 Linear scattering dichroism and relaxation rates (τ^{-1}) as a function of the field strength: $\Delta S = \Delta S_{\parallel} - \Delta S_{\perp}$, where $\Delta S_{\parallel}$ is the light intensity change observed with polarized light parallel to the direction of the applied electric field and $\Delta S_{\perp}$ is the signal of the perpendicular light polarization mode. See legend of Fig. 1. Note the positive value of ΔS of mode I and the negative value of ΔS of mode II. The relaxation rates of the conductivity relaxation mode I are the same as those of the optical model I, and the rates of mode III and the S(II) mode are roughly the same.

tially decaying forcing function, the subsequent conductance relaxations II and III.

Mode I of the light-scattering dichroism, defined as $\Delta S = \Delta S_{\parallel} - \Delta S_{\perp}$ (see Fig. 1), has the same relaxation rate (τ^{-1}) as the interfacial polarization current, at all field strengths (Fig. 2). The optical change thus seems to be caused by, and rate-limited by, the buildup of the electric potential difference across the membrane.

At higher field strengths a second relaxation with opposite amplitude compared to mode I is visible. This optical mode (II) is slightly faster than the relaxation mode (III) of the conductance relaxations, but both modes become observable at about the same field intensity, E_c of the 10-μs pulse.

B. Structural Changes

The conservative scattering dichroism suggests that the field-induced, interfacial ionic polarization of the vesicle causes solvent to enter the membrane. If these aqueous scattering centers are pores, the shape of the pore must be asymmetric as indicated by the light scattering anisotropy ($\Delta S \neq 0$). We may model these pores as narrow hydrophobic (HO) pores $(P_{HO})_r$ of radius r. If the field strength E reaches a critical value E_c at a given pulse duration Δt, a different pore quality appears. This pore type is associated with a negative value of the scattering dichroism and with a larger conductance. We model these pores as broader hydrophilic (HI) pores $(P_{HI})_{r>r_c}$, which are formed when a critical pore radius r_c is reached. The formation of these pores is slower ($\tau^{-1} = k_{HI} \approx 10^5\ s^{-1}$) compared to the HO pores ($\tau^{-1} = k_{HO} \approx 10^6\ s^{-1}$) because the transition $P_{HO} \rightleftharpoons P_{HI}$ involves rotation of lipid molecules in the pore wall.

1. Sequence of Membrane Changes

Since the light-scattering signal $\Delta S(I)/S(0)$ increases continuously with increasing field intensity, it is presumed that the number and size of hydrophobic (HO) pores increase continuously up to a saturation value (Fig. 2). The sequence of membrane changes from the poreless state (M) to HO pores $(P_{HO})_r$ and HI pores $(P_{HI})_r$ is modeled in Fig. 3.

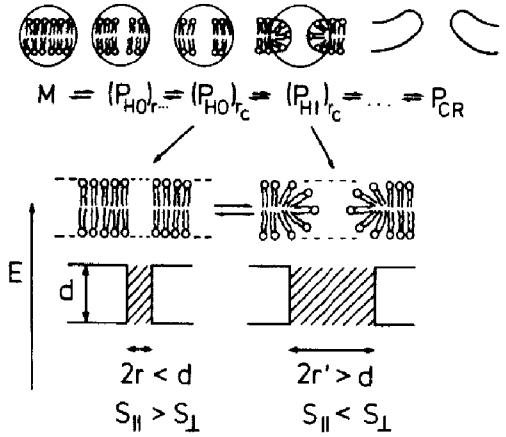

Figure 3 Sequence of events in membrane electroporation, modeled in terms of aqueous pores: M is the closed bilayer state, and $(P_{HO})_r$ is the hydrophobic pore of radius r. The HO pores convert to hydrophilic (HI) pores, $(P_{HI})_r$, if a critical radius r_c is reached; P_{CR} refers to crater-like pores. The geometrically anisotropic pores $2r \neq d$ describe the change of sign of the dichroitic signal $\Delta S = \Delta S_{\parallel} - \Delta S_{\perp} = S_{\parallel} - S_{\perp}$ with respect to the direction of the applied electric field E.

2. *Model for the HO ⇌ HI Transition*

For geometrical reasons of lipid packing, water will enter to a certain degree between the individual lipids of the pore wall of a hydrophilic pore. The transition

$$(P_{HO})_{r_c} \rightleftharpoons (P_{HI})_{r_c}$$

changes the geometry of the light scattering center. The HI pore ($2r' > d$) is broadened compared to the HO pore ($2r < d$); see Fig. 3.

3. *Field Strength and Pulse Duration*

The scheme of the structural transitions depicted in Fig. 3 is very instructive for the interpretation of the stimulus/duration curves: the higher the field strength, the shorter can be the pulse length in order to achieve the same membrane permeabilization. A low-intensity pulse may need a pulse duration of milliseconds to reach the same extent of structural transitions as a high intensity pulse applied for only microseconds. Thus even very small field intensities may cause DNA transfer, provided the field application is long enough (seconds). It is thus obvious that the specification of a critical field intensity E_c is only meaningful if the pulse duration Δt is also given.

4. *Pulse Number*

The return to the closed membrane state M (Fig. 3) after switching off the field at the end of the pulse occurs in the absence of the external field. In particular, the return transition $P_{HO} \leftarrow P_{HI}$, involving reorientation of the wall lipids, may face major activation barriers and thus is slow (seconds, minutes).

If now a second pulse hits the membrane patch not in the M state but in the remaining $(P_{HI})_r$ states, the change induced by the second pulse is facilitated, because the transitions $P_{HO} \rightarrow P_{HI}$ have already been caused by the first pulse. Thus in terms of membrane structure and lipid rearrangements the pulses of a pulse train are not equivalent.

III. Electroporation and Membrane Permeability

Among the various practical aspects, the electrotransformation of intact bacteria and other microorganisms requires media with low conductivity to reduce Joule heating, although that by itself can be favorable for efficient gene transfer (Wolf *et al.*, 1989). In any case, the interpretation of the low-conductivity data necessitates an extension of the analytical framework in terms of the external solution conductivity (Neumann and Boldt, 1989).

Using the green algae cells of the species *Chlamydomonas reinhardtii (Ch. reinh.)* as an example, a simple procedure is outlined to determine the critical electroporation voltage ($\Delta\varphi_{M,c}$) and the membrane/envelope conductivity (λ_m). Finally, a strategy is presented that permits the determination of optimum values of electric field strength, pulse length, and pulse number for the transient permeabilization of viable cells, thus providing a useful basis of optimization strategies for cell biological and medical applications.

A. Permeabilization–Resealing Cycle

It was recently recognized that the transient membrane electroporation may be viewed as a cycle of electropore formation and resealing resembling a relaxation hysteresis (Neumann, 1989). In brief, in the presence of the field pulse of limited duration (Δt = 5 μs to 10 ms), the cell membrane (initial states C, representing the actual state equilibria $M \rightleftharpoons \Sigma_r^{eq} (P_{HO})_r$) becomes more porous (states P representing the state equilibria $\Sigma_r^{eq}(P_{HI})_r$) and thereby also fusogenic. The state transitions $C \rightleftharpoons P$ in the presence of the electric field occur unidirectionally and may lead to irreversible rupture at long pulse durations. If, however, the electric field pulse is switched off before rupture or lysis of the cells occurs, the electropores or electrocracks anneal at $E = 0$, with $C \leftarrow P$ being unidirectional, too. The electroporation–resealing cycle may be represented by the scheme

$$C \underset{k_R}{\overset{k_P(E)}{\rightleftharpoons}} P \qquad (1)$$

where $k_P(E)$ and k_R are overall rate coefficients for electroporation and resealing, respectively. The electroporated (and fusogenic) membrane states P usually are long-lived, in particular at low temperatures (4°C).

If the electroporation hysteresis is coupled to other processes (states X), such as material release or uptake, or lysis, Scheme (1) has to be extended to

$$C \rightleftharpoons P \rightarrow\rightarrow X \qquad (2)$$

Usually for short pulse times Δt, the reverse transition $P \leftarrow C$ and the transition $P \rightarrow X$ occur at $E = 0$; they are after-field pulse effects.

B. Electrosensitivity

It is known that a biological cell population is inhomogeneous in cell size, in the state of growth, or in metabolic conditions. Nonspherical cells such as bacterium rods have different positions relative to the external electric field direction. Because of the dominantly negative surface charges of the cell wall, the rods will orient with their longest axis into the direction of the electric field. Both oriented rods and the

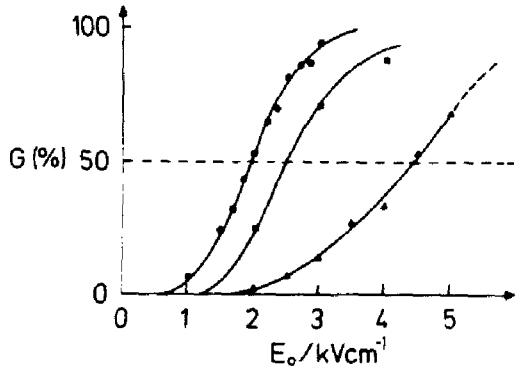

Figure 4 Electrosensitivity $G(\%)$ of a suspension of green algae cells *Chlamydomonas rheinhardtii* (wild type 11-32 c, Göttingen) to quasirectangular electric pulses of the initial field intensity E_0 and of the pulse length $\Delta t = 0.2$ ms at different medium conductivities λ_0: ●, $\lambda_0 = 3.5 \pm 0.1 \times 10^{-4}$ S cm^{-1}; ■, $\lambda_0 = 1.5 \pm 0.1 \times 10^{-4}$ S cm^{-1}; ▲, $\lambda_0 = 5.6 \pm 0.5 \times 10^{-5}$ S cm^{-1}. $G(\%)$ is the percentage of cells that were critically permeabilized such that the (lethal) dye serva blue G ($M_r = 854$, largest dimension 2.5 nm) was taken up, visibly coloring these cells.

oriented polyelectrolyte DNA will migrate with different velocities along the electric field lines. All these factors cause a distribution of the critical electroporation field strength E_c.

Figure 4 shows examples of such a distribution. Here, the state X in Scheme (2) is the colored cell (G), obtained by the uptake of a dye by the electroporated cell. The percentage $G(\%)$ of the G colored cells is given by: $G(\%) = 100 \times G/C_T$, where C_T is the total number of the cells. $G(\%)$ is a measure for the critically permeabilized cells.

For practical purposes we may take the field strength E_0 (50%) where $G(\%) = 50$ as representative for the cell population and define a mean value by

$$\bar{E}_c = E_0(50\%) \tag{3}$$

The width of the electrosensitivity of the cell population may be given in terms of a "variance" ($\pm \Delta\bar{E}_c$). Since E_c depends on the cell size, the mean value $\bar{E}_c$ corresponds to a mean value $\bar{a}$ of the effective radius of spherical cells. Here, too, we have a "variance": $\bar{a} + \Delta\bar{a}$.

C. Ionic Interfacial Polarization

The electroporation data suggest that the membrane electropermeabilization results from an indirect electric field effect. The structural changes of the membrane phase are preceded by the ionic interfacial polarization (Neumann, 1989).

Usually in electroporation experiments the polarization time constant τ_p (Schwan, 1957) is small compared with the pulse duration Δt, the buildup of the stationary value $\Delta\varphi(E)$ of the interfacial potential difference across the membrane is practically instantaneous.

For low-conductivity membranes of thickness d of cells of radius a, the stationary value is given by

$$\Delta\varphi(E) = -1.5f(\lambda)aE|\cos\delta| \tag{4}$$

where δ is the angle between the membrane site considered and the direction of E. The conductivity factor $f(\lambda)$ is a function of the specific conductances or conductivities of the external solution ($\lambda_0 \geqslant 10^{-4}$ S cm^{-1}), of the cell interior ($\lambda_i \approx 10^{-2}$ S cm^{-1}), and of the membrane ($\lambda_m \approx 10^{-7}$ S cm^{-1}), respectively, and of the ratio d/a.

Usually $\lambda_m \ll \lambda_i$, λ_0 and $d \ll a$ such that (Neumann, 1989)

$$f(\lambda) = [1 + \lambda_m(2 + \lambda_i/\lambda_0)/(2\,\lambda_i\,d/a)]^{-1} \tag{5}$$

If in low-conductivity media $\lambda_0 \ll \lambda_i$, but still $\lambda_0 \gg \lambda_m$, Eq. (5) reduces to a form that is particularly useful for graphical data evaluation:

$$[f(\lambda)]^{-1} = 1 + (\lambda_m a/2d)\,\lambda_0^{-1} \tag{6}$$

Obviously, E_c corresponds to a critical cross-membrane electroporation voltage $\Delta\varphi_{M,c}$; $\Delta\varphi_{M,c} \approx 1$ V (Sale and Hamilton, 1968) for short repetitive pulses of 20 μs. When the contributions of fixed surface charges and the associated ionic atmospheres can be neglected, the total trans-membrane voltage $\Delta\varphi_M(E)$ in the presence of the externally applied field E is a function of the intrinsic membrane potential $\Delta\varphi_m$ (e.g., $\Delta\varphi_m = -70$ mV) and of the interfacial polarization term $\Delta\varphi(E)$:

$$\Delta\varphi_M(E) = \text{fct}[\Delta\varphi_m, \Delta\varphi(E)] \tag{7}$$

The total potential profile in the direction of E is explicitly given by (Neumann, 1989)

$$\Delta\varphi_M(E) = -[1.5f(\lambda)aE + \Delta\varphi_m/\cos\delta]|\cos\delta| \tag{8}$$

Often $|\Delta\varphi(E)| > |\Delta\varphi_m|$, hence $\Delta\varphi_m(E) \approx \Delta\varphi(E)$. The pole caps of spherical membranes are the sites of maximum interfacial polarization. With $|\cos\delta| = 1$, Eq. (8) can be used to relate the mean values of $\bar{E}_c$ and $\bar{a}$ by the expression

$$\bar{E}_c = -\Delta\varphi_{M,c}/[1.5\bar{a}f(\lambda)] \tag{9}$$

Applying Eq. (6) for low-conductivity media we obtain

$$\bar{E}_c = -(\Delta\varphi_{M,c})/3\bar{a})[1 + (\lambda_m\bar{a}/2d)\,\lambda_0^{-1}] \tag{10}$$

When $\bar{a}$ is given by the geometrical radius of the most abundant cell size, the data in Fig. 5 can be used to determine $\Delta\varphi_{M,c}$ and λ_m. For the *Ch. reinh.* cells, $\bar{a} = 3.5$ μm: $\Delta\varphi_{M,c} = -0.8$ V, $\lambda_m \approx 5 \times 10^{-7}$ S cm^{-1}. The critical voltage 0.8 V at $\Delta t = 0.2$ ms compares well with the value of 1 V estimated by Sale and Hamilton

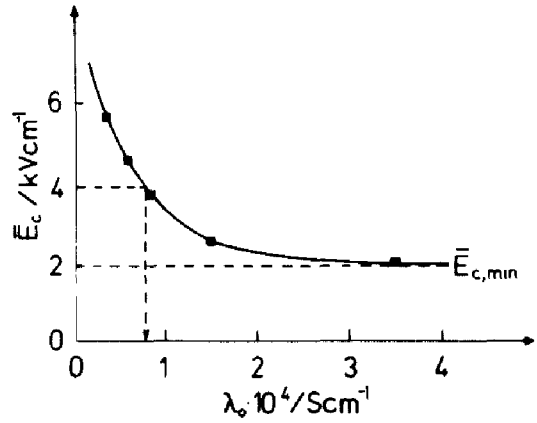

Figure 5 The population mean value $\bar{E}_c = E_0$ (50%) of *Ch. reinhardtii* cells (Fig. 4) decreases with increasing conductivities λ_0 of the pulsing medium. The λ_0 value at which $\bar{E}_c = 2\bar{E}_{c,min}$ [i.e., $f(\lambda) = 0.5$] is given by $(\lambda_0)_{0.5} = \lambda_m \bar{a}/2d$ and permits a simple graphical estimate of the λ_m value. From $\bar{E}_{c,min}$ we obtain $\Delta\varphi_{M,c} = -1.5a\bar{E}_{c,min}$.

(1968) for $\Delta t = 20$ μs. The dependence of E_c on λ_0 is quantitatively consistent with the concept of ionic interfacial polarization, being reduced at low medium conductivity (λ_0), that is, low electrolyte concentration. The data at low λ_0 values suggest that the membrane conductivity λ_m cannot be neglected; instead of $f(\lambda) = 1$, Eq. (6) applies.

D. Lifetime of Membrane Electroporation

The longevity of the electroporated cells is dependent on the temperature and may be measured by the after-plus addition of a dye (which colors the cell) at various times t_{add} after the electroporation pulse. Due to annealing processes more cells lose the permeability property at larger after-pulse addition times (Fig. 6). For the data analysis Scheme (2) is specified to

$$C \underset{k_R}{\overset{}{\rightleftarrows}} P \xrightarrow[k_D]{} G \qquad (11)$$

where k_R and k_D are the rate coefficients for resealing (R) and dye uptake (D) and X = G is the (lethally) colored cell state.

The data suggest that $k_D \gg k_R$, such that G is a quantitative measure of the cells in the critically electroporated states P ($= G$). The rate equation for Scheme (11) under these conditions is given by

$$-d[G]/dt = -d[P]/dt = -k_R[P] \qquad (12)$$

Integration for the boundary conditions $t = 0$: [P] = [P_0], and $t \to \infty$: [P] =

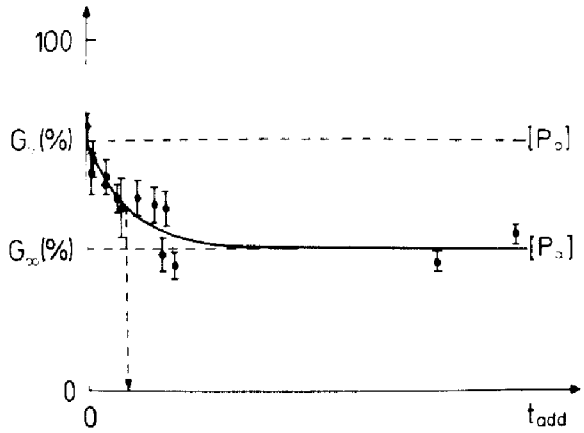

Figure 6 Time course of the recovery of the electroporated cells (resealing), measured by the uptake of the dye serva blue G, which was added at various times t_{add} after the electroporation pulse. For this example $k_R = 2.6\ (\pm\ 0.9) \times 10^{-2}\ s^{-1}$ at $T = 298$ K (25°C).

$[P_\infty]$ yields

$$[P(t)] - [P_\infty] = ([P_0] - [P_\infty]) \exp(-k_R t) \qquad (13)$$

Equation (13) permits the evaluation of the coefficient k_R of cell recovery from the observed exponential decay of $G(\%)$ in Fig. 6. Note that $G(\%)$ is proportional to P such that, for instance, $([P(t)] - [P_\infty])/([P_0] - [P_\infty]) = (G(t) - G_\infty)/(G_0 - G_\infty)$.

The rate coefficient k_R is a measure of the mean lifetime $\bar{t}_e$ of the electroporated cell state: $\bar{t}_e = k_R^{-1}$. In the example given in Fig. 6, $t_e \approx 40$ s; the electroporation state is thus called long-lived compared to the pulse duration of 0.2 ms (Fig. 4).

E. Physical Electroporation Parameters

The dye method of coloring electroporated cells can be used to determine the pulse strength–duration ($\bar{E}_c/\Delta t$) relationship and the dependence of $\bar{E}_c$ on medium conductivity (λ_0), on temperature, and on pulse number. The $\bar{E}_c/\lambda_0$ dependence yields λ_m as a membrane-specific electric parameter. By $G_m = \lambda_m/a$, the membrane conductance, G_m can be determined. For *Ch. reinh.*, $G_m \approx 1.4 \times 10^{-3}$ S cm^{-2}, comparing well with other biomembrane systems.

It is of particular practical importance that the values $G_0(\%)$ and $G_\infty(\%)$ can be used to determine, at a given pulse length and pulse number, the optimum range of E_0 for the electroporation experiments (Fig. 7). The optimum field strength range shifts when the medium conditions (λ_0, temperature, etc.) are changed; ΔE_0 and $\Delta G(\%) = G_0(\%) - G_\infty(\%)$ must be explored for every particular cell type.

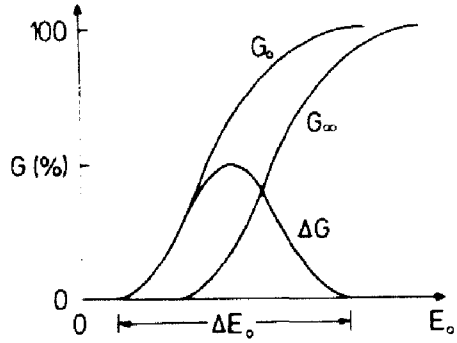

Figure 7 Scheme for the optimization of electroporation conditions; $\Delta G = G_0 - G_\infty$, representing the transiently permeabilized surviving cells. The field strength range ΔE_0 is shifted when the electroporation conditions are changed.

In summary, it is shown that the dye method, originally applied as a qualitative tool to estimate electroporated cells (Neumann *et al.*, 1980, 1982) can be quantified to yield useful information for the optimization of the electroporation technique.

IV. Electroporative DNA Transfer

One of the more recent developments in the technique of the electroporative gene transfer is the electrotransformation of intact bacteria, without pretreatment to remove the cell wall (see, for instance, Wolf *et al.*, 1989).

A. DNA Surface Adsorption

The number T of transformants per milliliter cell suspension increases with increasing DNA concentration [DNA] and with increasing cell density (Wolf *et al.*, 1989). Both correlations, T(DNA) at constant cell density and T(cell density) at constant DNA concentration, are of the Langmuir-type adsorption isotherm. We may model these observations with a scheme in which the electroporation hysteresis $C \rightleftharpoons P$ [see Eq. (1)] is coupled to the adsorptive, (electro)diffusive approach of DNA (D) to the surface of the cell (C), yielding the surface bound states $D \cdot C$ and $D \cdot P$:

$$\begin{array}{ccc} D + mC \rightleftharpoons D \cdot C & & \\ \Updownarrow \qquad \Updownarrow & & \\ D + mP \rightleftharpoons D \cdot P \leftrightarrow P \cdot D \rightarrow D_{in} \rightarrow TC & & \end{array} \qquad (14)$$

In Scheme (14), the process $D \cdot P \leftrightarrow P \cdot D$ denotes the crossmembrane transport of DNA, D_{in} is the DNA that entered the cytoplasm, and TC denotes transformed cell; m is the maximum number of surface binding sites for DNA per cell.

B. Analysis of DNA Surface Binding

It appears reasonable to assume that the probability of cell transformation increases with an increase in the concentration of the state D · P. If [TC] ~ [D · P], then

$$T/T_{max} = [TC]/[TC]_{max,} = [DP]/[DP]_{max} \tag{15}$$

In terms of Scheme (14) the extent of "adsorption" depends on DNA and cell concentration, respectively, according to

$$[DP]/[DP]_{max} = [D]/([D] + \bar{K}_D) = m[C]/(m[C] + \bar{K}_c) \tag{16}$$

where $\bar{K}_D = \bar{K}_c$ is given by

$$\begin{aligned} \bar{K}_D &= [D](m[C] + m[P])/([DC] + [DP]) \\ &= K_1(1 + K_0)/(1 + K_0') \end{aligned} \tag{17}$$

and $K_0 = [P]/[C]$, $K_1 = ([D]m[C])/[DC]$, $K_0' = [D \cdot P]/[D \cdot C]$, and $K_2 = K_1K_0/K_0'$ are the equilibrium constants of the individual steps.

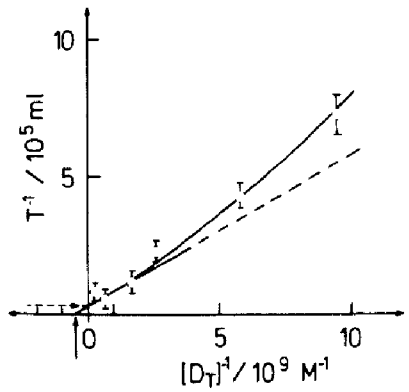

Figure 8 Electrotransformation of intact Corynebacterium glutamicum cells. Cell density 10^{10}/ml at 4°C. Quasirectangular pulse, $E_0 = 10$ kV cm^{-1}, $\Delta t = 5$ ms; medium: 0.272 *M* sucrose, 0.01 *M* HEPES buffer, 1 m*M* $MgCl_2$, KOH adjusted to yield pH 7.4 at 4°C, plasmid DNA pUL-330-plasmid (5.2 kb). The Langmuir adsorption type relationship between the number of transformants T per milliliter and the total concentration of DNA, $[D_T]$, is represented in terms of reciprocal quantities; $[T]^{-1} = T_{max}^{-1}(1 + \bar{K}_D/[D_T])$. The dashed line refers to the linear dependence on $[D]^{-1}$; [D] is the concentration of free DNA, $M = 3.43 \times 10^6$ g/mol. The abscissa and ordinate intercepts yield $\bar{K}_D = 2(\pm 1) \times 10^{-9}$ *M* (DNA) and $T_{max} = 3.3 \times 10^5$/ml.

Equations (15) and (16) can be combined and rewritten as

$$T^{-1} = T_{max}^{-1}(1 + \bar{K}_D/\{D\}) \qquad (18)$$

providing a convenient relationship for a graphical data evaluation. Note that [D] refers to the free, unbound DNA. The data representation in terms of the total DNA concentration $[D_T]$ is nonlinear in $1/[D_T]$, but it is suited to evaluate T_{max} and $\bar{K}_D$; see Fig. 8. For intact *Cornyebacterium glutamicum* cells we obtain $\bar{K}_D = 2(\pm 1) \times 10^{-9}$ *M*(DNA), $m = 25$, and $T_{max} = 3.3 \times 10^5$ ml^{-1} at $E = 10.5$ kV cm^{-1} and $\Delta t = 5$ ms.

The electroporative cell transformation of intact *Cornyebacterium glutamicum* cells can thus be quantitatively described in terms of preceding surface adsorption of the applied plasmid DNA.

Acknowledgments

We thank Mrs. M. Pohlmann for careful typing of the manuscript, the Deutsche Forschungsgemeinschaft for Grant Ne227/6–1 to E. Neumann, and the Fonds der Chemie.

References

Neumann, E. (1989). The relaxation hysteresis of membrane electroporation. *In* "Electroporation and Electrofusion in Cell Biology" (E. Neumann, A. E. Sowers, and C. A. Jordan, eds.), pp. 61–82, Plenum Press, New York.

Neumann, E., and Boldt, E. (1989). Membrane electroporation: biophysical and biotechnical aspects. *In* "Charge and Field Effects in Biosystems" (M. J. Allen, S. F. Cleary, and F. M. Hawkridge, eds.), Vol. 2, pp. 373–382, Plenum Press, New York.

Neumann, E., Gerisch, G., and Opatz, K. (1980). Cell fusion induced by high electric impulses applied to *Dictyostelium*. *Naturwissenschaften* 67, 414–415.

Neumann, E., Schaefer-Ridder, M., Wang, Y., and Hofschneider, P. H. (1982). Gene transfer into mouse lyoma cells by electroporation in high electric fields. *EMBO J.* 1, 841–845.

Neumann, E., Sowers, A. E., and Jordan, C. A. (eds.) (1989). "Electroporation and Electrofusion in Cell Biology." Plenum Press, New York.

Sale, A. J. H., and Hamilton, W. A. (1968). Effects of high electric fields on microorganisms. III. Lysis of erythrocytes and protoplasts. *Biochim. Biophys. Acta* 163, 37–43.

Schwan, H. P. (1957). Electrical properties of tissue and cell suspensions. *Adv. Biol. Med. Phys.* 5, 147–209.

Sowers, A. E. (ed.) (1987). "Cell Fusion." Plenum Press, New York.

Wolf, H., Pühler, A., and Neumann, E. (1989). Electrotransformation of intact and osmotically sensitive cells of *Corynebacterium glutamicum*. *Appl. Microbiol. Biotechnol.* 30, 283–289.